M. Effects of Highway Ice-Clearing Treatments on Corrosion of Heavy Vehicle Materials and Components

Principal Investigator: Elizabeth V. Stephens
Pacific Northwest National Laboratory
P.O. Box 999, Richland, WA 99352-0999
(509) 375-6836; fax: (509) 375-4448; e-mail: elizabeth.stephens@pnl.gov

Principal Investigator: Dane F. Wilson
Oak Ridge National Laboratory
P.O. Box 2009, Oak Ridge, TN 37831-8048
(865) 576-4810; fax: (509) 375-6605; e-mail: wilsondf@ornl.gov

Chief Scientist: James J. Eberhardt
(202) 586-9837; fax: (202) 587-2476; e-mail: James.Eberhardt@ee.doe.gov
Field Technical Manager: Philip S. Sklad
(865) 574-5069; fax:(865) 576-4963; e-mail:skladps@ornl.gov

Participants:
Stan Pitman, Karl Mattlin, Mike Dahl, and Clyde Chamberlin, Pacific Northwest National Laboratory
Claire Luttrell, Peter Blau, and Ed Kenik, Oak Ridge National Laboratory

---

Contractors: Pacific Northwest National Laboratory, Oak Ridge National Laboratory
Contract No.: DE-AC06-76RL01830, DE-AC05-00OR22725

Objective

- Evaluate the corrosion that may be associated with the various ice-clearing chemical systems that are in use by the various states and regions for snow and ice control.
- Develop a more fundamental understanding of the interaction of these chemicals with representative heavy vehicle materials and structures.
- Develop a unified modeling procedure to represent "rust jacking" (displacement of brake friction materials) caused by stresses induced by corrosion products at the interface of the brake shoe and the friction liner.

Approach

- Evaluate heavy truck corrosion damage to identify materials, components, and safety-related systems affected by anti-icing/deicing treatments.
- Identify and characterize $MgCl_2$ solutions and corrosion-inhibiting additives.
- Perform accelerated corrosion testing and corrosion characterization of heavy vehicle materials.
- Evaluate brake shoe failures to identify aggressive corrosion species and extent of corrosion.
- Determine the thermo-elastic and mechanical properties of the lining material, brake shoe table, and corrosion products.
- Incorporate the mechanical properties of the lining material, brake shoe, and corrosion products into computer-aided engineering (CAE) codes to predict the stresses associated with swelling of oxides on the shoe/lining interface.
- Identify more desirable ice-clearing chemical formulations and application methods.

- Generate “best practice” recommendations for reduced vehicle corrosion and improved safety.

Accomplishments

- Conducted in-service winter field evaluations in collaboration with Montana Department of Transportation (Phase 2 – Winter Season 2004/05).
- Characterized the effects of $MgCl_2$ anti-icing/deicing solutions and other ice-clearing chemical products on heavy vehicle materials (Phase 1).
- Prepared specimens with "lip" for demonstrating moisture retention time effects and added specimens to the field evaluation.
- Began accelerated corrosion testing of heavy vehicle materials.
- Conducted forensic analysis of failed brake shoes.
- Determined the remainder of the thermal and mechanical properties of the brakes.
- Evaluated the stresses that arise from the growth of corrosion products between the pads and the brake table
- Completed model of brake “rust jacking”.

Future Direction

- Complete analysis of corrosion field evaluations (Phase 2).
- Complete assessment of Boeing’s anti-icing technologies for heavy vehicles and trailers for the elimination of ice and ice-clearing chemical accumulation.

Introduction

In recent years, many states have introduced anti-ice liquid treatments, particularly $MgCl_2$ road treatments, to prevent the bonding of ice and snow before the onset of a winter storm. Spraying the treatment on roads before the onset of a storm potentially exposes vehicles to concentrated solutions for longer periods of time because the solution is not immediately diluted by snow or water. Increased corrosion damage to heavy truck components has been reported by truck fleets and owner/operators. Vehicle safety concerns have arisen, including accelerated corrosion damage in heavy truck brake systems, also known as “rust jacking” (Figure 1).

Although there is a strongly voiced opinion within the trucking community that accelerated damage is being caused by $MgCl_2$ road treatments, there is a lack of significant data to quantify the role of various $MgCl_2$ treatments on heavy truck component corrosion.

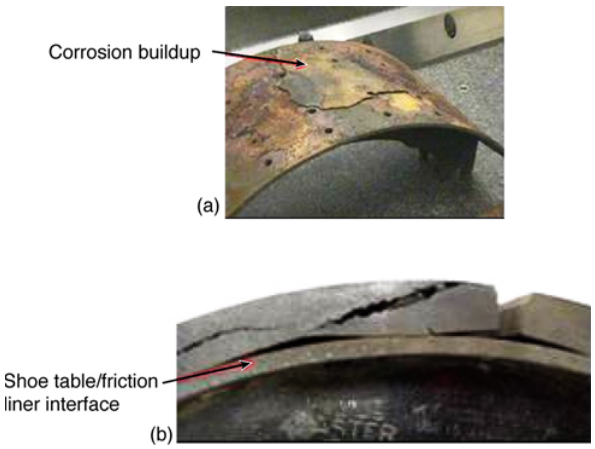

Figure 1. An illustration of rust jacking: (a) corrosion product buildup on the brake shoe table displaces the brake lining; (b) shoe table/friction liner interface.

In May 2003, Pacific Northwest National Laboratory and Oak Ridge National Laboratory began collaboration on a 2-year research effort focused on developing a more fundamental understanding of the interaction of these chemicals with representative heavy vehicle materials and structures.

Corrosion Field Evaluation

The corrosion field evaluation, in collaboration with the Montana Department of Transportation (MDT), continued for the 2004/05 winter season. The remaining corrosion coupon panels were removed in May 2005. Chrome-plated steel, 1008 steel with a lip, and stainless steel coupons have been added to the evaluation. These coupons will also be evaluated and compared with those removed at the end of the 2003/2004 winter season. In addition, a new exposure region was added to the evaluation to include corrosion-inhibited sodium chloride as the sole chemical used. Again, corrosion coupon racks were placed on select MDT liquid-dispensing and abrasive trucks that were exposed to different ice-clearing chemicals and winter conditions in various regions throughout western Montana (Figure 2).

Figure 2. An illustration of the seven urban regions in Montana.

The field evaluation continued in Utah for the 2004/2005 winter season. To include NaCl exposure as part of the test matrix, the Utah Department of Transportation allowed MDT to place four corrosion coupon racks on its liquid dispensing and abrasive trucks (also designating a region as the sole chemical used). Coupon racks also remained on one commercial hauler traveling the United States to include a national, mixed exposure to ice-clearing chemicals.

Winter Season 2003/2004 Phase 1

Last season, aluminum alloy 5182-O, cast aluminum A356, and 1008 steel corrosion coupons were exposed to approximately 4-5 months of ice-clearing chemicals. The coupons were exposed to the following ice-clearing chemical combinations:

- Corrosion- inhibited $MgCl_2$ only
- Corrosion- inhibited $MgCl_2$ and NaCl solid
- Corrosion- inhibited CaCl and NaCl solid
- NaCl solid or brine only
- Mixed exposure

The coupons were evaluated to determine the corrosion observed and a general corrosion rate. To date, no localized corrosion or pitting was observed on the 1008 steel and A356 cast aluminum specimens. Only general uniform corrosion was observed.

However, inter-granular corrosion was observed on all 5182-O specimens, regardless of exposure type. Mg_2Al_3 precipitates form a continuous path along the grain boundaries. Since, Mg_2Al_3 is a highly anodic second phase that is present, it corrodes preferentially and a selective attack of the grain boundary is observed. Figure 3 is representative of the corrosion observed on the aluminum specimens.

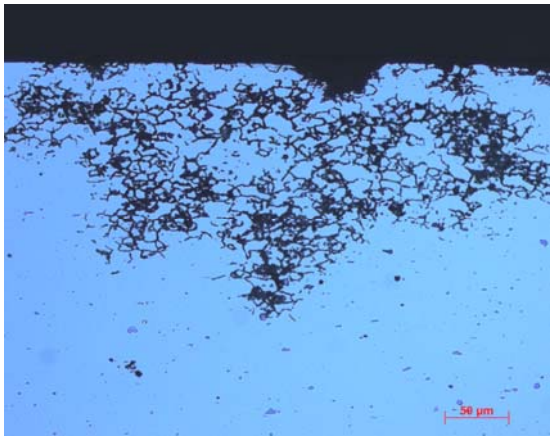

Figure 3. Photo representative of the inter-granular corrosion attack observed on 5182-O aluminum specimens from the field.

Corrosion rates were determined for each coupon specimen to evaluate the differences in corrosion behavior when exposed to different ice-clearing chemicals. The corrosion rate in mils penetration per year was determined by the following equation:

$$MPY = \frac{534W}{DAT}$$

where *W* is the weight loss in milligrams, *D* is the density in grams per cubic centimeter, *A* is the exposed area in square inches, and *T* is the exposed time in hours.

Figure 4a-c illustrates the corrosion rate results for each coupon material. Slightly varying trends were observed for each material alloy in regards to the region and chemicals it was exposed to. For instance, lower corrosion rates were observed for both 1008 steel and A356 cast Al specimens when exposed to a $MgCl_2$ in comparison to NaCl. However, lower corrosion rates were observed in 5182-O specimens that were exposed to NaCl in comparison to $MgCl_2$.

One trend that is dominant across all the alloys evaluated is larger corrosion rates typically observed in regions where both $MgCl_2$ and NaCl are being utilized. Further investigation of the quantities of materials used in each region and differences in exposure time and exposure truck mileage is needed to better understand the trends observed. In addition, further investigation of the effect of chloride content and/or cations present is needed. Correlation between the trends observed and previous electrochemical tests conducted that studied the anion and cation effect are needed.

Quasi-static tensile tests were conducted on several of the corrosion coupons received from Phase 1 to quantify the effect of the corrosion behavior observed on the structural integrity of the material. One inch by four inch strips were prepared from the corrosion coupons. Moderately corroded specimens were compared to severely corroded specimens (determined by corrosion rate). A non-exposed specimen was used as a baseline. In general, a decrease in strength was observed in corroded specimens ranging from approximately 3%-12% depending on corrosion severity and alloy type. Figure 5 illustrates the static results observed for 5182-O aluminum specimens. Further tensile tests are currently being conducted on all coupons from each varying exposure type, and region, to further assess the preliminary results.

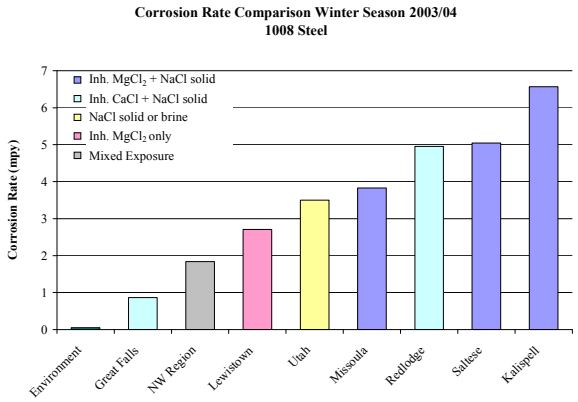

(a)

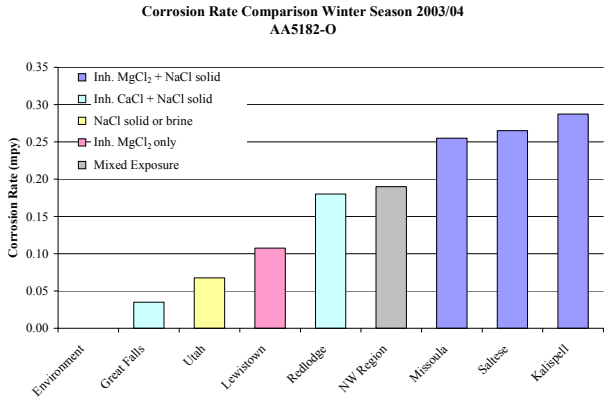

(b)

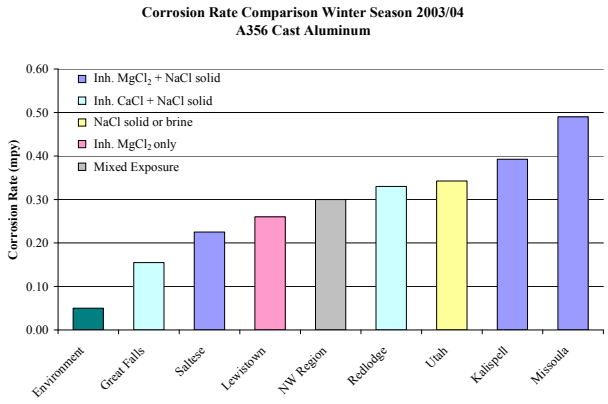

(c)

Figure 4. The corrosion rate results to date for the corrosion coupons removed from each region and varying exposure type. (a) 1008 steel specimen results. (b) 5182-O specimen results. (c) A356 cast Al specimen results.

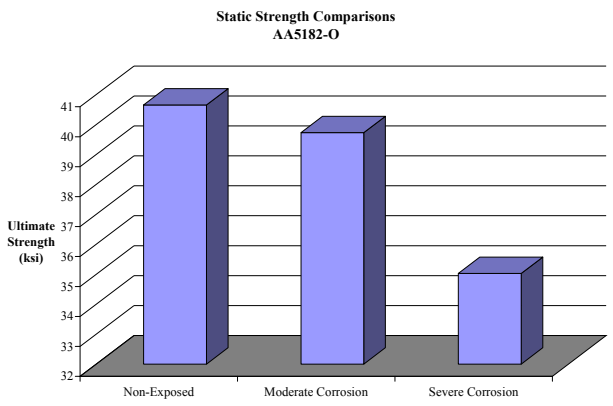

Figure 5. Illustration of the static test results for corroded 5182-O specimens from the field.

Accelerated Corrosion Laboratory Tests

Alternate immersion tests and SAE J2334 cyclic tests are currently being conducted. Figure 6 illustrates the alternate immersion set up and specimen design. Crevice washers were also utilized to study the effects of crevice corrosion.

The corrosion behavior of the specimens from each test will be correlated with the corrosion coupons from the field.

The alternate immersion tests are being conducted at 50ºC and 90% relative humidity, and at 0ºC, no humidity. The cyclic tests involve a humid stage at 50ºC and 100% humidity, a 15 minute salt application, and a dry stage at 50ºC. Four different deicer exposures are being conducted and seven alloys are being investigated. They include the following:

- 1008 steel,
- 304 stainless steel
- Chrome plated steel (cyclic tests only)
- 5182-O aluminum
- 5052-H32 aluminum
- 6061-T6 aluminum
- A356 cast aluminum

The alternate immersion tests at 50ºC and 90% humidity have been completed. Evaluation of the specimens is ongoing. General uniform corrosion has been observed in the 1008 specimens. Localized pitting and possible intergranular corrosion has been

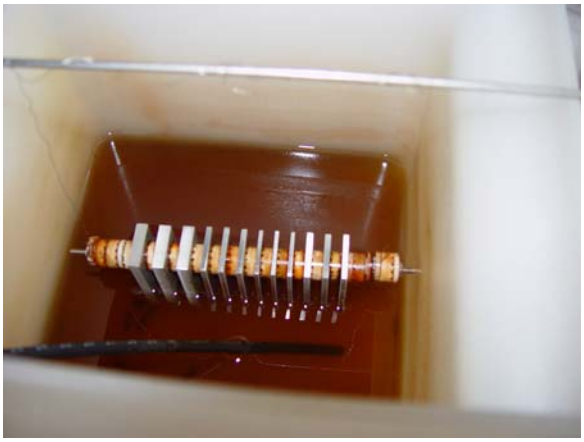

(a)

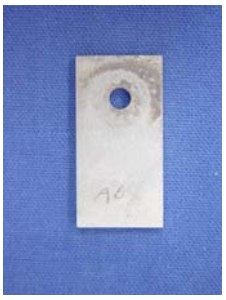

(b)

Figure 6. (a) The alternate immersion test set up and (b) specimen design.

observed in the A356 aluminum castings, and possible pitting has been observed in the 5182-O specimens. Further evaluation of all specimens is needed.

Modeling of Brake Lining Failure

A model of the brake lining material fracture phenomenon, caused by the forces produced by the growth of corrosion products at the shoe table/lining interface, has been developed. The mechanical properties of the lining material and oxides determined experimentally have been incorporated into analysis codes to predict the stresses associated with swelling of oxides on the shoe/lining interface.

Flexure Tests

Flexure tests have been completed on the brake pad material at room temperature, 100, 200, and 400°C. The results of these tests have been used to determine the modulus of elasticity for the finite element analyses of the brake lining model.

Modeling Efforts

Finite-element techniques have been used to predict stresses on the back side of the lining associated with swelling of oxides in the shoe/lining interface. Lining and oxide property data determined experimentally have been used as inputs for the model. Initially, two-dimensional (2D) analyses were used to determine the effects of oxide particles of different sizes inserted between the brake shoe and lining. The particle was assumed to be in the shape of half an ellipse. The major diameter of the oxide particles was assumed to be 3.2 mm. The minor radius, or height, of the half-ellipse was varied.

The first analysis assumed the assembly was at room temperature. The stresses due to a particle with a height of 0.4 mm, inserted in the center of the pad, were calculated. The results of this analysis are shown in Figure 7.

These stresses exceeded the strength of the pad material. The location of this particle was changed to compare the stresses with the oxide particle at another location. Since the lining is stiffer where the rivets are closer together, the particle was moved to a location where the rivets are closer together. The stresses due to the same size particle are higher for the second case. Figure 8 shows the results of this analysis.

Other analyses were performed assuming particle heights of 0.2 mm and 0.1 mm, located between the closely spaced rivets. The analyses were done at room temperature and assumed that the entire assembly was at 100ºC. The results were compared with the strength of the lining at the given temperature. It was determined that a particle with a height as small as 0.1 mm could cause the lining to crack. An additional calculation was conducted to more accurately determine the temperature distribution in the brake assembly. The results of this analysis show that although the temperature on the surface of the lining may be high, the low thermal conductivity of the lining material keeps the shoe/lining interface temperature low. With this temperature profile, an additional stress calculation was done with the 0.1-mm-high particle. The results of all these analyses are shown in Table 1.

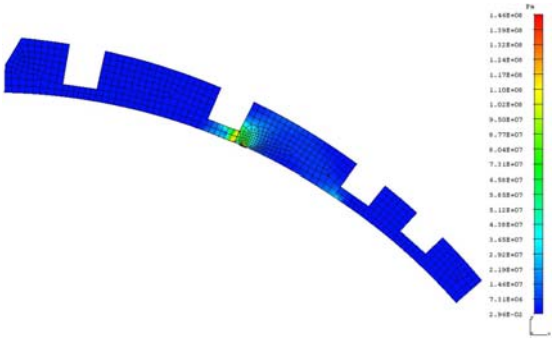

Figure 7. Stresses in the brake lining with the oxide particle located in the middle of the lining.

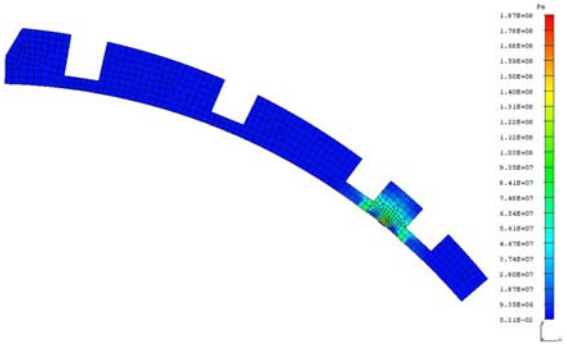

Figure 8. Stresses in the brake lining with the oxide particle located where rivets are close together.

Table 1. Results of 2D stress analyses.

Height (mm)	Temp (ºC)	Pad peak stress (MPa)	Strength (MPa)
0.4	RT	187	40.39
0.4	100	105	17.82
0.2	RT	93	40.39
0.2	100	52	17.82
0.1	RT	47	40.39
0.1	100	26	17.82
0.1	Temp profile	46	40.39

After examining the effect of oxide particle size and location with a 2D model, a 3D model was developed to include the actual assembly configuration. A 2D model assumes that the rivets fix the lining to the shoe in a line, rather than just at the rivet location. This makes the structure stiffer than it actually is. An analysis was done with an oxide particle with a height of 0.1 mm inserted between the rivets, as in the 2D analysis. The results of this case show that the stresses are actually less

than were calculated in the 2D analysis. The results of this case are shown in Figure 9.

The finite element analyses of the brake lining/shoe assembly show that a particle with a height of 0.1 mm will exert stresses on the lining that are close to the strength of the material. A larger particle would cause stresses that exceed the material strength. The analyses show that the worst location for the oxide particles is in the stiff regions of the lining around the rivets. Other areas of the shoe can have larger oxide layers. Although the analyses show that the stiffer regions are more likely to fail, this does not take into account all the factors. The other areas, with fewer rivets, may allow more corrosive chemicals between the lining and shoe and therefore may have more corrosion. This could cause failure in those areas first.

Additional analyses were performed as a function of the major diameter or width of the oxide particle, the shape of the particle (elliptical to flat), the location of the particle, and the distance the particle covers into the brake shoe.

The width of the elliptical shaped oxide particle was varied from 3.2 mm to 14 mm. The 14 mm particle covered most of the area between the rivets as shown in Figure 10.

The results of these analyses showed that for any shape of the particle between the closely spaced rivets, the height of the oxide particle is the primary contributor to the stresses in the brake pad. These results are presented in the first four rows of Table 2. In row five, the results for the flat oxide particle (located as shown in Figure 10) with the height reduced to 0.08 mm is presented. The oxide particle for this case has a width of 14 mm and the length of 25.4 mm. Around the rivet holes, 0.08 mm is the limiting height before the strength of the pad is exceeded.

Analyses were performed for particles located away from the rivet holes. An oxide particle with a height of 0.1 mm, a width of 14 mm and a length of 25.4 mm was placed in the middle of the brake pad, as shown in Figure 11.

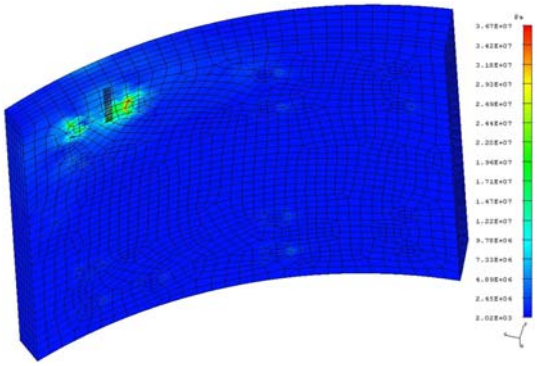

Figure 9. Brake lining stresses at interface for 3D analysis.

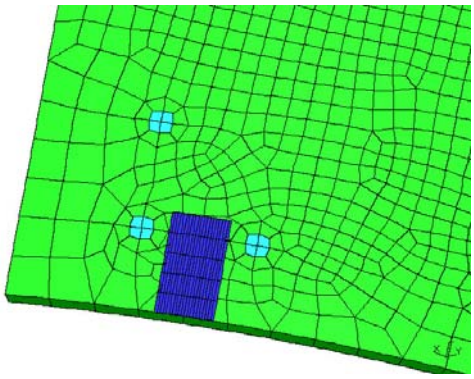

Figure 10. Model illustrating three rivets and a long wide particle.

Table 2. Predicted peak stresses for various particles.

Height (mm)	Width (mm)	Length (mm)	Shape	Peak Pad Stress (MPa)
0.10	3.2	25.4	Elliptical	45.1
0.10	8	25.4	Elliptical	45.3
0.10	14	25.4	Elliptical	47.6
0.10	14	25.4	Flat	47.7
0.08	14	25.4	Flat	39.2
0.10	14	25.4	Flat	5.46
0.20	14	25.4	Flat	34.9
0.10	14	62	Flat	43.7

The results for this case showed that the flexibility of the pad away from the holes allows an oxide particle located away from the hole to have a larger height than around the rivets. The results, presented in rows 6 and 7 of Table 2, show that the peak stresses due to a particle 0.2 mm high, away from the rivets, are below the strength of the pads. As the

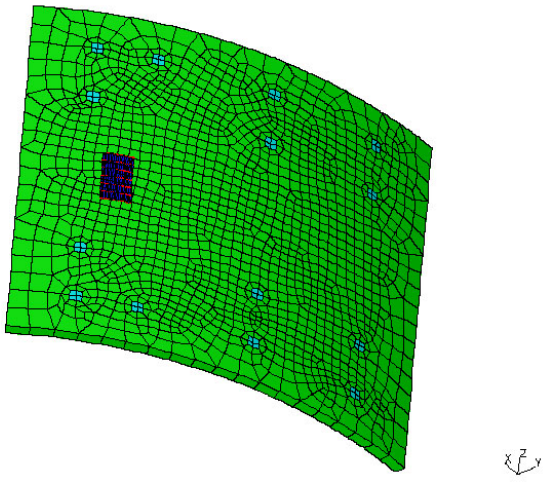

Figure 11. Model illustrating small oxide particle located between two rivets.

length of the oxide particle is extended toward the rivets, as shown in Figure 12, the stresses in the pads exceed the strength of the material. The peak stress in this case is presented in the last row of Table 2.

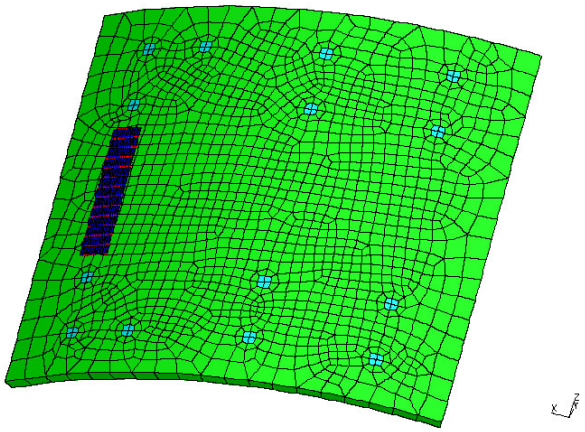

Figure 12. Model illustrating longer oxide particle located between two rivets.

Conclusions

- Intergranular corrosion occurred in all 5182-O Al coupons from the field regardless of exposure type.
- A significant corrosion effect being observed from field coupons exposed to both $MgCl_2$ and NaCl.
- For coupons that were severely corroded from the field, a ~10-12% reduction in strength was observed for 5182-O Al and 1008 steel specimens, ~6% reduction for A356 cast Al specimens.
- Different corrosion behaviors are observed from field coupons in comparison to lab tested coupons for 5182-O Al and A356 cast Al specimens to date.
- Determined that 0.10 mm oxide creates force larger than brake pad strength.
- Determined no difference in the layered corrosion products of brake tables exposed during operations to de-icing compounds with/or without $MgCl_2$.
- Demonstrated that a small amount of corrosion leads to large stresses in the brake lining.

Presentations

During this reporting period, three presentations were made to the following organizations:

- Montana Dept. of Transportation – December 6, 2004.
- Corrosion Forum, Western Transportation Institute, Montana State University- December 7, 2004.
- 21st Century Truck Partnership Project Review Meeting, Oak Ridge, TN - September 14, 2005.